International Journal of Radiation Biology

ISSN: (Print) (Online) Journal homepage: https://www.tandfonline.com/loi/irab20

Investigation of radiation protective features of azadispiro derivatives and their genotoxic potential with Ames/*Salmonella* test system

Burak Alaylar, Bünyamin Aygün, Kadir Turhan, Mehmet Karadayı, Esra Cinan, Zuhal Turgut, Gökçe Karadayı, Mohammed Ibrahim Abu Al-Sayyed, Medine Güllüce & Abdulhalik Karabulut

To cite this article: Burak Alaylar, Bünyamin Aygün, Kadir Turhan, Mehmet Karadayı, Esra Cinan, Zuhal Turgut, Gökçe Karadayı, Mohammed Ibrahim Abu Al-Sayyed, Medine Güllüce & Abdulhalik Karabulut (2022): Investigation of radiation protective features of azadispiro derivatives and their genotoxic potential with Ames/*Salmonella* test system, International Journal of Radiation Biology, DOI: 10.1080/09553002.2022.2087930

To link to this article: https://doi.org/10.1080/09553002.2022.2087930

Published online: 25 Jul 2022.

Submit your article to this journal

Article views: 64

View related articles

View Crossmark data

Full Terms & Conditions of access and use can be found at
https://www.tandfonline.com/action/journalInformation?journalCode=irab20

INTERNATIONAL JOURNAL OF RADIATION BIOLOGY
https://doi.org/10.1080/09553002.2022.2087930

Taylor & Francis
Taylor & Francis Group

ORIGINAL ARTICLE

Check for updates

Investigation of radiation protective features of azadispiro derivatives and their genotoxic potential with Ames/*Salmonella* test system

Burak Alaylar[a], Bünyamin Aygün[b], Kadir Turhan[c], Mehmet Karadayı[d], Esra Cinan[e], Zuhal Turgut[c], Gökçe Karadayı[f], Mohammed Ibrahim Abu Al-Sayyed[g,h], Medine Güllüce[d], and Abdulhalik Karabulut[e]

[a]Department of Molecular Biology and Genetics, Faculty of Science and Arts, Agri Ibrahim Cecen University, Agri, Turkey; [b]Department of Electronics and Automation, Vocational School, Agri Ibrahim Cecen University, Agri, Turkey; [c]Department of Chemistry, Faculty of Art and Sciences, Yildiz Technical University, Istanbul, Turkey; [d]Department of Biology, Faculty of Science, Atatürk University, Erzurum, Turkey; [e]Department of Physics, Faculty of Science, Atatürk University, Erzurum, Turkey; [f]Department of Molecular Biology and Genetics, Faculty of Science, Atatürk University, Erzurum, Turkey; [g]Department of Physics, Faculty of Science, Isra University, Amman, Jordan; [h]Department of Nuclear Medicine Research, Institute for Research and Medical Consultations (IRMC), Imam Abdulrahman bin Faisal University (IAU), Dammam, Saudi Arabia

ABSTRACT

Purpose: Five different types of synthesized azadispiro derivatives have been analyzed for radiation absorption capacity and determined their potential to be exploited as substances for a drug to be developed against radiation has been investigated.

Material and methods: Fast neutron attenuation parameters like the effective mean free path, half-value layer (HVL), removal cross-sections, and neutron transmission number were found with the Monte Carlo simulation Geometry And Tracking (GEANT4) code. Gamma radiation absorption parameters, such as effective atom number (Z_{eff}), mean free path (MFP), mass attenuation coefficient (MAC), and half-value layer (HVL) were theoretically determined with WinXCom software. Besides, the exposure build-up factor (EBF) was calculated by using GP fitting parameters. Neutron absorption dose rate was experimentally calculated with ^{241}Am-Be fast neutron source which has 4.5 MeV of energy, 74 GBq activity, and portative BF_3 neutron detector. Ames/*Salmonella* test systems were used for the genotoxic potentials of the azadispiro derivatives

Results and conclusions: Experimental and theoretical results were checked with paraffin and High-Density Polyethylene. The results showed that Azadispiro derivatives have neutron radiation absorption capability close to paraffin and High-Density Polyethylene. The gamma radiation absorption properties for azadispiro derivatives have been investigated, and it has been observed that these materials can absorb gamma radiation. Ames/*Salmonella* assay was used to examine whether the derivatives had a genotoxic effect probability or not. The results showed that these derivatives were genotoxic and safe at test doses (up to 5 mM). Consequently, it has been understood that these azadispiro derivatives can be used as active and genotoxic safety ingredients in the production of a protective drug against both neutrons and gamma rays.

ARTICLE HISTORY
Received 9 March 2022
Revised 12 May 2022
Accepted 14 May 2022

KEYWORDS
Azadispiro derivatives; radiation; genotoxicity; Ames test system; drugs

1. Introduction

Radiation (neutron, gamma, X-Ray, etc.) have a crucial role in various type of fields, such as electricity generation, medicine, agriculture, archaeology, geology, industry, laboratory, and space research for the benefit of humanity (USNRC 2017). In addition to these benefits of radiation, exposure to radiation for a short time depending on its energy can lead to health problems, such as acute radiation syndrome and skin burns. If exposed to radiation at high energy levels for a long time, it may cause diseases, such as cancer and cardiovascular (Dauer et al. 2017). The best way to protect workers and those living in the environment from the harm of radiation is to use protective materials. For this purpose, many types of research are made every day and new materials are successfully developed. Many different materials, polymers (Aygün et al. 2015; Aygün et al. 2020a; More et al. 2021), glasses (Kaewkhao et al. 2017; Aygün et al. 2020b), heavy concrete (Sayyed and Lakshminarayana 2018; Aygün et al. 2021a), alloys (Aygün et al. 2019; Ekinci et al. 2019) have been developed. It is easy to stop the radiation outside, but when it enters the human body, it is very difficult to reduce the damage it causes. As a result of a nuclear accident or war, radioactive particles, such as iodine 131 can cause various risk factors by entering the human body. In such a situation, there is a great need for drugs that can protect cells, hold radiation, and repair cells to protect cells and tissues from radiation. It showed the need for an effective anti-radiation drug after the accident at the Fukushima nuclear power plant in Japan. Anti-radiation drugs can prevent the damage caused to tissues and cells by the incoming

CONTACT Bünyamin Aygün baygun@agri.edu.tr Department of Electronics and Automation, Vocational School, Agri Ibrahim Cecen University, Agri, Turkey

Copyright © 2022 Taylor & Francis Group LLC.

radiation of the human body, reduce the clinical symptoms of radiation-induced diseases and accelerate the healing (Tan et al. 2016). In addition to the studies carried out for this purpose, new research is being carried out every day. Currently, potassium iodide (KI) is a non-radioactive iodine salt and is widely used commercially as an anti-radiation drug. This drug is produced in the United States of America (USA) by Anbex and Fleming Pharmaceuticals companies, which have been approved by the Food and Drug Administration (FDA). This salt is used to protect against radioactive iodine that can enter the thyroid glands. Moreover, the polysaccharide is a polymer formed by the binding of 10 or more monosaccharides found in the structures of plants, animals, and microorganisms with glycosidic bonds (Tang et al. 2017). It has been determined that polysaccharides have physiological functions, such as anti-radiation antioxidant, immunoregulation, and tumor inhibition. It has also been reported that polysaccharides do not have a toxic effect on tissue cells and do not lower blood sugar (Feng et al. 2013). Again, in some studies, polysaccharides have been shown to be protective against radiation, and it was stated that this could be used in the development of a drug against radiation (Wang et al. 2020). In another research, the anti-radiation effect of oleuropein was investigated and human mononuclear cells were coated with an optimum concentration of 100 µM and then irradiated with gamma radiation with 2 Gy energy. It was determined then by (3-(4,5-dimethylthiazol-2-yl)-2,5-diphenyltetrazolium bromide (MTT) test that oleuropein protects cells and has an anti-radiation property (Amani et al. 2021).

Spiropiperidine derivatives, which form the core of the alkaloid and natural product family with strong medicinal and interesting structural properties, have a significant position in the field of heterocyclic chemistry. These compounds, often situated in many natural and synthetic products and beneficial biopharmaceuticals, are potent-receptor ligands, epileptic disorders, bad cocaine abuse, depression, and 5-HT_{2B} receptor (5-hydroxytryptamine receptor 2B) antagonists. The presence of piperine motifs in drug molecules has recently been the focus of scientific studies in the development of effective protocols because of their crucial role in pharmacological profile, such as selective and strong effect.

Since spiro compounds have many uses, synthesis studies have been continuing recently. Most of the spiro compounds are anticancer (Reddy et al. 2011; Erugu et al. 2014; Das et al. 2020) anticonvulsants (Kesharwani et al. 2009; Zaher et al. 2010), antibacterial (Youssef and Amin 2010) anti-Alzheimer's (Kamiński et al. 2008), antituberculosis (Al Houari et al. 2008), anti-dermatitis (Yoshikawa et al. 2009), analgesic and antimicrobial (Srivastava et al. 2020). In addition, these compounds are also used in industry and agriculture (Thadhaney et al. 2010). On the other hand, the quinoline derivatives were synthesized and their genotoxic potentials in both radiation levels were determined and studies have shown that these syntheses can be used for a protective drug that can be developed for both gamma and neutron radiation (Aygün et al. 2021c; Alaylar et al. 2021).

In this study, five different types of azadispiro derivatives and their experimental and theoretical neutron and gamma absorption capacities ability were determined. Then, Ames/*Salmonella* test system was carried out to investigate of genotoxic safety of these azodispro derivatives. It has been clearly understood that azadispiro derivatives can be considered and used for promising drug substances against radiation.

1.1. Radiation absorption theory

The neutron cross-section is aimed to search the probability of interactions that may occur between the neutron entering a target material and the core of the target material. These interactions usually include elastic and inelastic or nuclear reactions, such as neutron capture, fission, and spallation. Barn (10^{-28} m^2 or 10^{-24} cm^2), which is accepted as the standard unit, is used to indicate this cross-section of interaction. These cross-sections are mostly determined with total macroscopic cross-section and the removal cross-section value is found as follows. The large total or removal cross-section of this cross-section expresses the high probability of interaction that the neutron coming to the material can make with the nucleus of the material (El-Khayatt and El-Sayed Abdo 2009). Any interaction of neutrons with the target material can be defined in different cross-sections as below.

σ_α; (n, α) reaction cross-section, σ_p; (n, p) reaction cross-section, σ_T; (n, T) reaction cross-section. σ_Υ; radiative capture cross-section, σ_i; inelastic scattering cross-section, σ_e; elastic scattering cross-section, σ_f; fission scattering cross-section,

By the results, neutron absorption cross-section (1), scattering cross-section (2), and total cross-section (3) are designated as below.

$$\sigma_a = \sigma_\gamma + \sigma_f + \sigma_T + \sigma_p + \sigma_\alpha \quad (1)$$

$$\sigma_s = \sigma_i + \sigma_e \quad (2)$$

$$\sigma_t = \sigma_a + \sigma_s \quad (3)$$

The macroscopic cross-section ($\sum_t$) shows the area of interaction of all nuclei in the total volume of the target material, but expressed in cm^{-1} units and figured out as below (Lamarsh and Baratta 2001):

$$\Sigma = N\sigma \ (cm^{-1}) \quad (4)$$

$$N = \frac{\rho}{A} N_A \quad (5)$$

where N is the atomic density in the interaction sample, ρ is the density of the interaction sample, and N_A is Avogadro's number.

The total macroscopic cross-section can be figured out for samples, as follow:

$$\Sigma_t = \Sigma_i N_i (\sigma_t)_i \quad (6)$$

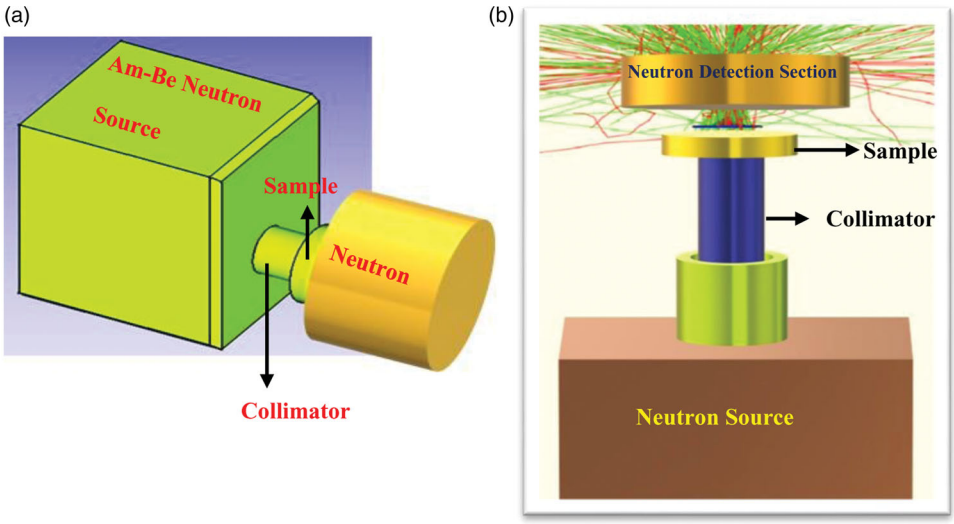

Figure 1. (a) Experimental geometry with experimental dose measurements. (b) 3-D view of the GEANT 4 simulation geometry set up to calculate the shielding parameters of all samples.

where N_i is the number of (nuclei density) are nuclei/m^3, and $(\sigma_t)_i$ is the total microscopic cross-section of the ith target material (Tsoulfanidis 1984).

Another parameter that is widely used in the attenuation of fast neutrons is the effective removal cross-section. The probability of neutrons having a fast or fission energy level to make the first collision after entering the target material is determined by this cross-section and this cross-section is figured out below (Tellili et al. 2014).

$$\sum_R = \sum_i \rho_i \left(\sum_R / \rho\right)_i \tag{7}$$

$$\rho_i = \omega_i \rho \tag{8}$$

where ω_i is the weight fraction and ρ_i is the fractional density (gcm^{-3}) of the ith component material.

HVL refers to the material thickness that can absorb 50% of the total amount of radiation on the target matter and is an important criterion in radiation shielding applications figured out below (Zali et al. 2018).

$$HVL = \ln 2 / \Sigma R \tag{9}$$

The MFP shows the average distance a neutron particle interacting with the material can travel through the material without being absorbed and is figured out as below (McAlister 2016).

$$\lambda = {}^1/_{\sum_t} \tag{10}$$

when gamma rays react with a target substance, they scatter or pass through the substance in accordance with the Beer-Lambert law given below.

$$I = I_0 e^{-\mu x} \tag{11}$$

where x is the material thickness (I_0); attenuated gamma rays (I); attenuated gamma rays, μ is the linear attenuation coefficient (LAC).

MAC of substance can be found in the LAC number value divided by the density number value of the sample. The material thickness that reduces the intensity of gamma rays by 50% on the target material is defined by HVL and it can be found as follow (Şakar et al. 2020).

$$HVL = \frac{\ln(2)}{\mu} \tag{12}$$

$$MFP = \frac{1}{\mu} \tag{13}$$

The effective atomic number gives information about the radiation behavior of a complex material, which varies according to the energy of the radiation interacting with the material, and this value is a virtual atomic number calculated as follows.

$$Z_{eff} = \frac{\sum_i f_i A_i (\mu/\rho)_i}{\sum_i f_i A_i Z_i^{-1} (\mu/\rho)_i} \tag{14}$$

where f_i, Z_i, and A_i are the mole fraction, atomic number, and atomic mass of the ith consistent elements.

Z_{eq} is using a parameter that defines the containing several ingredients materials characteristic in terms of equivalent elements like atomic the number for a single element. The parameter is given info about photoelectric absorption and the photon removal processes and pair production, it is calculated as follows (Sayyed et al. 2017).

$$Z_{eq} = \frac{Z_1 \ (logR_2 \ - logR) + Z_2 (logR - logR_1)}{logR_2 - logR_1} \tag{15}$$

where Z_1, Z_2 are the atomic numbers and the ratios R_1, R_2 of elements in the examined sample. R is the ratio for the azadispiro derivatives at a certain energy. R is the ratio of Compton partial mass attenuation coefficients ($\mu_{compton}$) to the total mass attenuation coefficients (μ_{total}).

2. Material and methods

2.1. Monte Carlo simulation code GEANT4

The Geometry And Tracking (GEANT4) is a Monte-Carlo simulation kit that can simulate the reactions that may arise

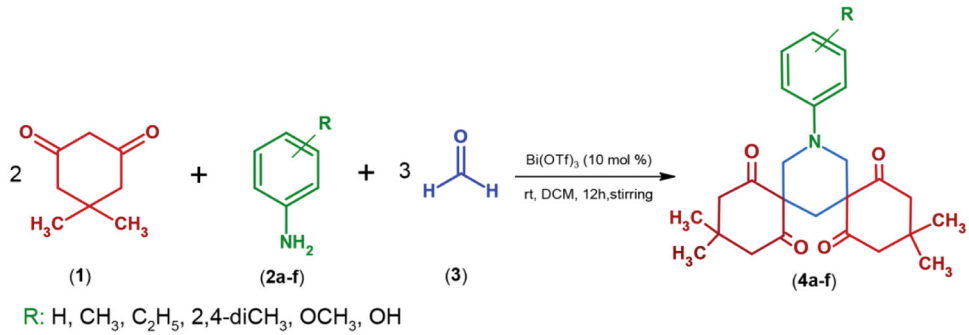

Figure 2. General schematic presentation of synthesis of bis-spiropiperidine derivatives using $Bi(OTf)_3$ as the catalyst. Reagents and conditions: dimedone **1** (2 mmol), substituted aniline **2a–f** (1 mmol), formaldehyde **3** (3 mmol), $Bi(OTf)_3$ (10% mol), 12 h stirring at room temperature.

during the passage of charged particles and radiation via matter. It has been utilized in various disciplines, such as radiotherapy, particle and nuclear physics, reactor and detector design, and space research. In this study, the events that may arise during the passage of neutrons via target materials are determined by the simulation given in Figure 1. In these simulations, parameters like transmission number, effective removal sections, average free path, and half-value thickness were calculated.

2.2. General procedure for the synthesis of 3,3,11,11-tetramethyl-15-(substituted phenyl)-15-azadispiro[5.1.5.3]hexadecane-1,5,9,13-tetrone derivatives and test sample preparation for neutron radiation experiments

Aromatic amines (1 mmol) were added to the solution of dimedone (2 mmol), and formaldehyde (3 mmol) formed in dichloromethane (DCM) under the catalysis of $Bi(OTf)_3$ and at room temperature for 12 h to obtain 3,5-dispiro-substituted piperidine compounds from the three-component condensation (Figure 2). Thin-layer chromatography (TLC) was carried out to monitor the proceeding of the reaction. Then, the reaction was completed, and a thick precipitate was acquired. The crude solid product was filtered, and oven-dried. The crude product was purified by column chromatography using an n-hexane/ethyl acetate (2:1) mixture. Spectroscopic methods were carried out to characterize pure products. The physical and chemical features of the synthesized substances are given in Tables 1 and 2. Spirocyclisation proceeds as a domino sequence of Knoevenagel, Michael, and Mannich reactions. The most important reasons for prefer to this method are including beneficial properties, such as being eco-friendly, non-toxic, efficient, and inexpensive. Five different types of synthesized azadispiro derivatives (AD1–5), the chemical content and features are given in Table 1, and the synthesized scheme is shown in Table 2. The sample preparation of neutron radiation experiments was carried out as follows, the solid azadispiro derivatives were dissolved in dimethyl sulfoxide (DMSO). Then, the derivatives were added to the melted agarose solution (1.5% w/v in DMSO at 50 °C). The final concentration was adjusted as 5 mM for each derivative, and 10 mL of the adjusted mixture was transferred into a Petri dish (60 × 15 mm) and solidified. The same procedure was carried out for the control group without the addition of any azadispiro derivative. In the experiments performed to define the fast neutron absorption capacities of the samples, neutron source, and dosimetry system acquired from Canberra Industries (Meriden, Connecticut-United States), the properties of which are shown in Table 3, ^{241}Am-Be fast neutron source with 74 GBq activity and average energy of 4.5 MeV and CANBERRA NP series neutron detector (BF_3 gas) were used. As given in Figure 1(a), whole matters were located in front of the neutron source and bombarded for 25 min. First, the unprotected dose (D_0) was detected by calculating the dose from the neutron source.

The protected dose (DD) passing through the sample in front of the source was figured out. After, the amount of dose absorbed for each material was calculated via equation ($D = D_0 - D_D$). According to these results, in Table 4 by using Equation $(D/D_0) \times 100$, an experimental dose absorbed rate (%) was figured out.

2.3. Preparation of test samples for neutron radiation experiments

Five different types of synthesized azadispiro derivatives (AD1–5), the chemical content and features are given in Table 1, and the synthesized scheme is shown in Table 2. The solid azadispiro derivatives were dissolved in dimethyl sulfoxide (DMSO). Then, the derivatives were added to the melted agarose solution (1.5% w/v in DMSO at 50 °C). The final concentration was adjusted as 5 mM for each derivative, and 10 mL of the adjusted mixture was transferred into a Petri dish (60 × 15 mm) and solidified. The same procedure was carried out for the control group without the addition of any azadispiro derivative.

2.4. Ames/Salmonella assay

2.4.1. Tester strains and chemicals

The tester strains *Salmonella typhimurium* TA97a, TA98, TA100 from Moltox® Inc., Boone (NC, USA) and TA1535, and TA1537 were provided from The American Type Culture Collection (ATCC®), Bacteria Department of Georgetown University (Washington-USA). The stock solutions were stored at −87 °C for further studies. For Ames/Salmonella assay, the working cultures were obtained from

Table 1. Chemical compositions of synthesized bis-spiro piperidine derivatives, their structures elucidated by spectroscopic methods, and their densities calculated in Chemdraw Pro 12.0 program (this study).

Sample code	Structure of compound	Molecular weight (g/mol)	Molecular formula	Composition (%)	Density (g/cm^3)
AD1	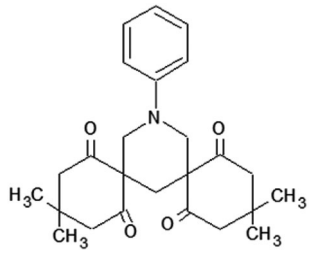	409.51794	$C_{25}H_{31}NO_4$	C: 73.32 H: 7.63 N: 3.42 O: 15.63	1.20 ± 0.1
AD2	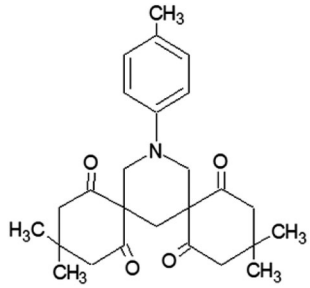	423.54452	$C_{26}H_{33}NO_4$	C: 73.73 H: 7.85 N: 3.31 O: 15.11	1.19 ± 0.1
AD3	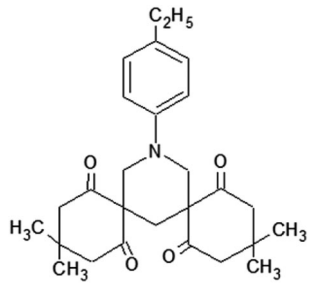	437.5711	$C_{27}H_{35}NO_4$	C: 74.11 H: 8.064 N: 3.20 O:14.63	1.17 ± 0.1
AD4	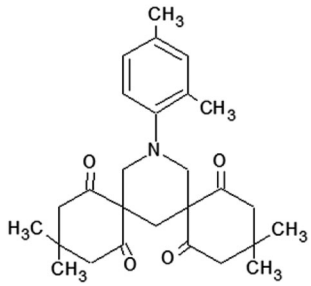	437.5711	$C_{27}H_{35}NO_4$	C: 74.11 H: 8.06 N: 3.20 O: 14.63	1.18 ± 0.1
AD5	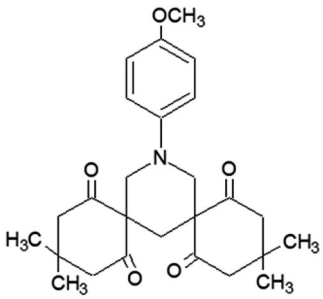	439.54392	$C_{26}H_{33}NO_5$	C: 71.05 H: 7.54 N: 3.19 O: 18.20	1.21 ± 0.1

Table 2. IUPAC (International Union of Pure and Applied Chemistry) nomenclature, starting components and % yields of synthesized compounds (this study).

Entry	Ar	Product	Name of product	Yield %
AD1	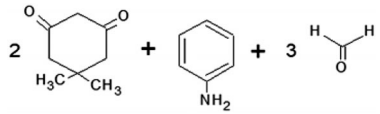	AD1	3,3,11,11-Tetramethyl-15-phenyl-15-azadispiro[5.1.5.3]hexadecane-1,5,9,13-tetraone	65
AD2	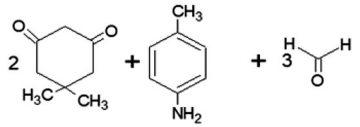	AD2	3,3,11,11-Tetramethyl-15-(4-methylphenyl)-15-azadispiro[5.1.5.3]hexadecane-1,5,9,13-tetraone	86
AD3	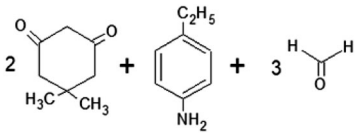	AD3	3,3,11,11-Tetramethyl-15-(4-ethylphenyl)-15-azadispiro[5.1.5.3]hexadecane-1,5,9,13-tetrarone	81
AD4	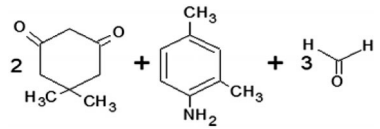	AD4	3,3,11,11-Tetramethyl-15-(2,4-dimethylphenyl)-15-azadispiro[5.1.5.3] hexadecane-1,5,9,13-tetraone	74
AD5	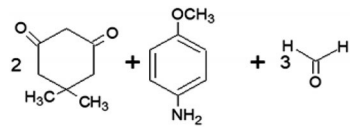	AD5	3,3,11,11-Tetramethyl-15-(4-dimetoxyphenyl)-15-azadispiro[5.1.5.3]hexadecane-1,5,9,13-tetraone	83

the stock solutions and inoculated into a nutrient broth medium for incubation at 37 °C an overnight (Tuğcu et al. 2018). Besides, 9-aminoacridine (9-AA), 4-nitro-o-phenylenediamine (4-NPD), and sodium azide (NaN_3) were bought from ABCR GmbH & Co. KG (Karlsruhe, Germany) as a positive control for direct-acting mutagens. The other reagents and solvents required for Ames/*Salmonella* assay were provided by Sigma–Aldrich® (St. Louis, MO, USA).

Table 3. Nuclear structure properties of the ^{241}Am-Be neutron source (Alaylar et al. 2021).

Physical half-life: 432.2 years, specific activity: 127 GBq/g			
Principle emissions	Energy (MeV)	Effective energy (MeV)	Dose rate (Sv/h/GBqat1m)
Gamma	0.0139 (42.7%), 0.0595 (35.9%)	–	85
Alpha	5.4430 (12.8%), 5.4860 (85.2%)	–	–
Neutron	–	4.5	0.6

Table 4. Experimental absorbed dose results of the samples (Aygün et al. 2021b).

Sample	Absorbed dose by samples (μSv/h)	Absorbed dose rate experimental
Background	0.9838 ± 0.098	–
P.	0.3125 ± 0.021	31.76%
HDPE	0.3020 ± 0.032	30.69%
AD1	0.2649 ± 0.025	26.92%
AD2	0.2805 ± 0.029	28.51%
AD3	0.2801 ± 0.026	28.47%
AD4	0.2819 ± 0.028	28.65%
AD5	0.2568 ± 0.027	26.10%

P: paraffin; HDPE: high density polyethylene; AD: azadispiro derivatives.

2.4.2. Detection of applicable concentrations of test compounds

The concentrations of the azadispiro derivatives on the *S. typhimurium* tester strains were carried out by using Turhan et al.'s (2012) protocol. Thus, it was clearly understood that the related tested concentrations exploited in the current experiment did not possess any harmful side effects on the test strains.

2.4.3. In vitro genotoxicity assays

Ames/*Salmonella* assay was exploited to define the genotoxic potentials of the azadispiro derivatives as test strains. The assessment of genotoxic usage of test strains was carried on according to the Mortelmans and Zeiger (2000) protocol. The method is one of the most well-known techniques for the identification of the genotoxic potential of the various type of tester compounds. According to the assay; 4-NPD (2.5 μg/plate) for TA97a and TA98, NaN_3 (5 μg/plate) for *S. typhimurium* TA100 and TA1535, and 9-AA (50 μg/plate) for *S. typhimuriu*m TA1537. 10% DMSO was exploited as a negative control for all tester strains. As the first step of the experiment, 100 mL of the liquid bacterial cultures and 50 mL of the test compound solution increased, respectively from 1 to 5 mM/plate, and then the compounds were put in

Table 5. Ames/*Salmonella* bacterial reversion assay results of the test compounds.

		Number of revertant colonies for *S. typhimurium* tester strains* (Mean ± S.D.)				
Test compound	Concentration (mM/plate)	TA1535	TA1537	TA97a	TA98	TA100
AD1	2	36.83 ± 2.79	23.67 ± 0.82	38.33 ± 3.83	24.83 ± 3.06	44.83 ± 4.71
	4	36.00 ± 3.41	27.83 ± 1.47	38.17 ± 2.64	26.17 ± 2.99	48.17 ± 3.66
	6	36.00 ± 2.37	26.50 ± 2.07	39.33 ± 2.50	24.83 ± 2.56	43.17 ± 2.15
	8	34.50 ± 3.33	26.33 ± 1.86	40.50 ± 3.56	24.00 ± 3.52	46.67 ± 1.21
	10	36.33 ± 3.83	25.17 ± 1.72	38.83 ± 3.31	23.33 ± 3.78	48.00 ± 3.22
AD2	2	36.67 ± 3.93	24.00 ± 1.55	39.67 ± 3.20	25.33 ± 2.34	42.83 ± 3.37
	4	36.17 ± 3.54	26.67 ± 1.37	40.17 ± 3.06	26.83 ± 1.33	47.00 ± 2.76
	6	35.67 ± 3.50	26.50 ± 1.64	38.67 ± 3.20	24.00 ± 2.10	46.67 ± 2.94
	8	37.67 ± 3.93	26.83 ± 2.71	42.00 ± 1.10	24.67 ± 3.39	45.67 ± 4.80
	10	35.50 ± 4.32	26.83 ± 2.40	40.17 ± 3.71	25.83 ± 3.87	45.50 ± 3.33
AD3	2	34.00 ± 3.03	26.00 ± 2.45	40.50 ± 2.88	23.50 ± 1.87	44.17 ± 2.04
	4	35.83 ± 3.66	25.50 ± 2.43	41.00 ± 2.00	24.83 ± 3.54	44.33 ± 3.44
	6	31.50 ± 2.35	26.17 ± 2.48	40.83 ± 3.66	24.17 ± 3.19	46.67 ± 2.58
	8	37.50 ± 2.26	26.50 ± 1.64	38.83 ± 4.07	27.50 ± 1.38	43.67 ± 2.07
	10	38.00 ± 3.22	27.17 ± 2.32	41.83 ± 3.06	26.00 ± 3.10	46.17 ± 2.99
AD4	2	33.83 ± 4.22	26.17 ± 2.56	41.33 ± 1.75	23.17 ± 1.60	47.50 ± 3.56
	4	34.50 ± 3.33	25.33 ± 2.88	39.50 ± 2.59	25.50 ± 2.88	45.33 ± 4.80
	6	35.67 ± 4.18	26.17 ± 1.94	38.83 ± 2.79	25.83 ± 2.64	41.50 ± 1.64
	8	35.67 ± 3.27	26.50 ± 1.87	39.17 ± 2.99	24.83 ± 3.49	45.17 ± 2.14
	10	36.17 ± 2.23	27.00 ± 1.79	40.50 ± 3.83	25.00 ± 2.83	43.83 ± 4.62
AD5	2	34.67 ± 4.18	25.67 ± 2.50	39.00 ± 2.97	26.33 ± 3.01	44.33 ± 2.58
	4	34.33 ± 3.27	25.50 ± 2.43	40.67 ± 3.01	25.17 ± 2.40	42.50 ± 2.26
	6	35.00 ± 3.90	24.83 ± 1.60	38.83 ± 2.14	26.83 ± 1.33	45.83 ± 3.87
	8	36.33 ± 2.73	25.33 ± 2.25	39.00 ± 3.85	22.33 ± 2.88	44.67 ± 4.27
	10	36.17 ± 3.43	26.50 ± 2.17	39.67 ± 3.44	26.17 ± 3.31	43.83 ± 3.31
Positive C.						
NaN_3	5 μg/plate	335.00 ± 9.06				555.50 ± 9.57
9-AA	50 μg/plate		256.17 ± 4.45	479.0 ± 10.53		
4-NPD	2.5 μg/plate				319.83 ± 5.98	
Negative C.						
DMSO	100 μl/plate	34.67 ± 4.13	26.00 ± 2.76	36.83 ± 3.13	24.67 ± 2.80	45.50 ± 2.95

*The results are presented as the mean and standard deviation of three experiments with two replica.

Table 6. Cytotoxicity assay results of the test compounds on the tester strains.

	Colony numbers on nutrient Agar plates for 10^{-5} dilution (Means ± S.D.)				
Test groups	TA1535	TA1537	TA97a	TA98	TA100
Control (DMSO)	632.7 ± 7.8	532.0 ± 7.1	608.8 ± 4.9	575.5 ± 7.2	512.2 ± 5.4
AD1 (10 mM)	636.5 ± 7.4	537.2 ± 9.1	618.3 ± 4.6	571.3 ± 6.0	520.8 ± 10.6
AD2 (10 mM)	627.3 ± 8.5	528.8 ± 7.4	614.7 ± 10.2	568.8 ± 15.7	515.2 ± 14.3
AD3 (10 mM)	636.0 ± 10.6	534.7 ± 5.6	614.3 ± 10.3	574.5 ± 10.8	514.7 ± 14.2
AD4 (10 mM)	627.3 ± 12.4	528.0 ± 10.8	615.0 ± 10.5	571.2 ± 12.1	519.8 ± 12.9
AD5 (10 mM)	628.8 ± 12.9	533.2 ± 9.0	619.7 ± 8.4	572.7 ± 13.2	512.8 ± 11.5

Significant reduction in cell survival was not detected.
Observations also confirmed that there was normal growth of the background lawn and the spontaneous colony numbers were within the regular range.

500 mL of sodium-phosphate buffer solution, then 2 mL of the top agar completed with 0.5 mM histidine/biotin was transferred to the mixture. The mixture was rapidly poured onto minimal glucose agar (MGA) solid media and incubated at 37 °C for 48 h. After the incubation step, the bacterial colonies were counted which is formed by the histidine-independent revertant. The counting results were analyzed by using the plate incorporation method (Maron and Ames 1983). According to these results mutagenic index was calculated for each dose of azadispiro derivatives with the following equation: $MI = R_{TC}/R_{NC}$.

According to the formula, the mutagenic index is containing to RTC (which represents the average count of the histidine independent revertant), and RNC (the average number of revertants in the negative control). Test materials with an increase at twice as much dose-related increase in the number of returned colonies are considered genotoxic. ANOVA and Student's test were used for the statistical analysis of the finding of three experiments with a triplicate plate/dose experiment. The result were given in Tables 5 and 6.

3. Results

3.1. Neutron absorption parameters

In the present study, five distinct synthesized azadispiro derivatives were studied according to their radiation absorption capabilities and genotoxic potential. Initially, neutron attenuation parameters, such as effective removal cross-section ΣR (cm^{-1}), MFP, HVL, and transmission number were theoretically carried out by using the Monte Carlo simulation Geant4 code which the organized in Figure 1(b). The detailed information were exhibited in Table 7 and Figure 3. To determine the absorption capabilities of the samples, the results were compared with both paraffin and high-density polyethylene, which are commonly exploited in neutron shielding treatments. It is clear from the simulation results that the synthesized azadispiro derivatives have high ΣR (cm^{-1}) and low HVL, MFP, and transmission values.

Neutrons are particle-type radiation, and the number of these particles interacting with the target material is expressed in flux per unit volume. Hence, the number of these neutrons interacting with the target material can provide information about the stopping ability of that material (Schober 2014). Samples were bombarded with 1×10^6 neutrons to define the number of neutron particles passing through all samples. As seen in this Table 7, the number of neutrons passing through the synthesized Azadispiroes is close to the reference samples. In a conclusion, it can be said that these samples have good absorption ability.

Table 7. Comparison of azadispiro derivatives fast neutron shielding parameters (Aygün et al. 2021c).

Sample code	Half value layer (mm)	Mean free path λ (mm)	Transmission number-GEANT4
P	60.761 ± 0.210	9.756 ± 0.412	902497
HDPE	60.910 ± 0.201	9.970 ± 0.130	904544
AD1	70.566 ± 0.211	10.917 ± 0.106	912420
AD2	70.492 ± 0.208	10.810 ± 0.260	911617
AD3	70.533 ± 0.201	10.869 ± 0.230	912020
AD4	70.476 ± 0.205	10.787 ± 0.270	911384
AD5	70.591 ± 0203	10.952 ± 0.260	912672

P: paraffin; HDPE: high density polyethylene; AD: azadispiro derivatives.

3.2. Experimental dose measurement results

Using the experimental set-up equation $D = D_0 - D_D$ given in Figure 2, the absorbed dose of all samples was determined. Experimental absorption dose measurements of five of the synthesized Azadispiro derivatives (AD1, AD2, AD3, AD4, and AD5) and reference samples were performed. First, the dose from the source was measured as 0.9838 μSv/h. Experimental absorption dose amounts are given in Table 4. From this table, the absorption dose rates with a dose of 0.9838 (μSv/h) from the neutron source by Azadispiro derivates (AD) samples are equal to 26.92% (AD1), 28.51% (AD2), 28.47% (AD3), 28.65% (AD4), and 26.10% (AD5). Paraffin and HDPE (High-Density Polyethylene) selected as reference samples absorbed 31.76 and 30.69% radiation, respectively. These results are not much higher than the Azadispiro derivatives studied.

3.3. Gamma radiation shielding properties

Gamma radiation shielding parameters, such as MAC, Z_{eff}, HVL, and MFP were calculated theoretically by using WinXCom software in the energy range from 0.015 to 15 MeV (Gerward et al. 2004). In addition, the exposure buildup factors (EBF) of azadispiro samples were calculated by using GP fitting parameters. The variation of the MAC values calculated for the investigated samples *vs.* the photon energy is shown in Figure 4. It is seen clearly from this graph that the MAC values for all samples decrease sharply

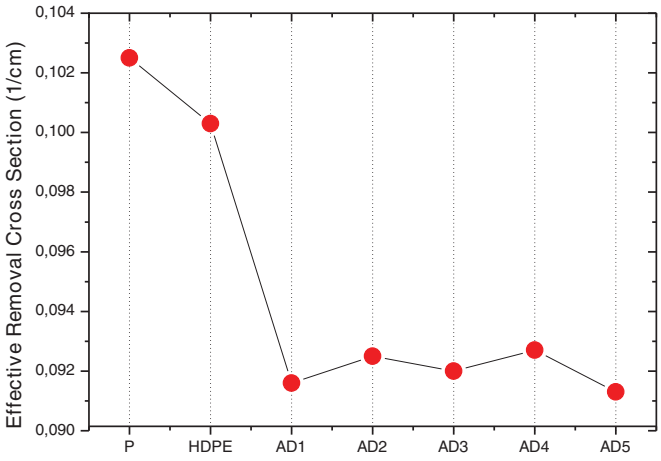

Figure 3. Comparison of effective removal cross-section shielding parameter values of all samples.

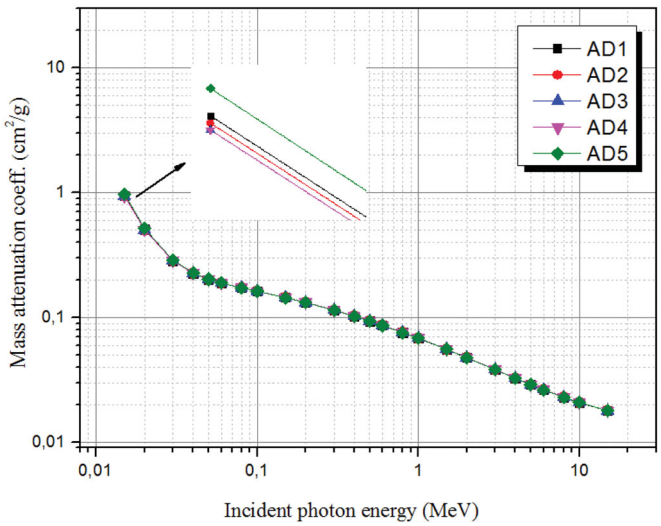

Figure 4. Comparison of MAC shielding values for all azadispiro samples with different contents in the energy range of 0.015–15 MeV.

depending on increasing photon energy in low-energy regions.

Z_{eff} is one of the most important gamma-ray shielding interaction properties, as it provides information about a composite's environment when interacting with a gamma-ray (Singh et al. 2007). Z_{eff} values of the studied samples were calculated by using the Equation (14). Figure 5 shows the Z_{eff} variation for these samples *vs.* the photon energy. Decrease order of Z_{eff} values at all photon energy regions is observed as AD3 = AD4 < AD2 < AD1 < AD5.

HVL is an important photon-matter interaction parameter since it remarks the thickness needed to reduce the radiation level to half of its initial value in designing any radiation shielding (Biswas et al. 2016). In addition, this parameter is used to determine the progression criteria of photons that interact with chemical compounds in a tissue or body in medical applications (Alaylar et al. 2021; Aygün et al. 2021c). HVL values were calculated by using MAC values and density values in this study and the variation of these values *vs.* the photon energy is presented in Figure 6.

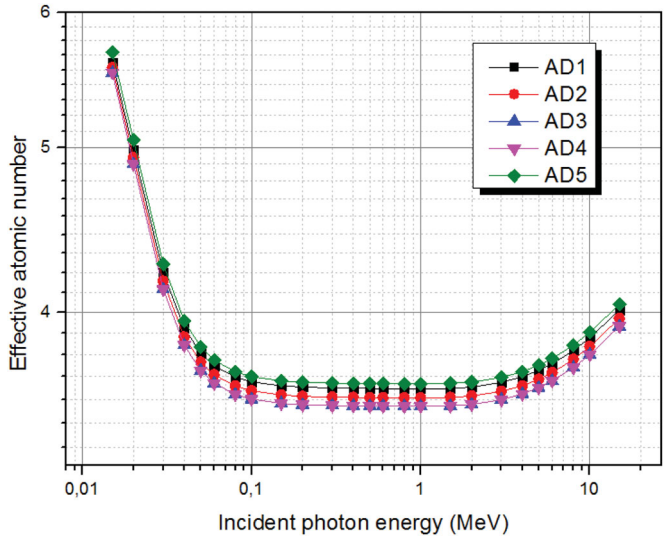

Figure 5. Comparison of Z_{eff} shielding values for all azadispiro samples with different contents in the energy range of 0.015–15 MeV.

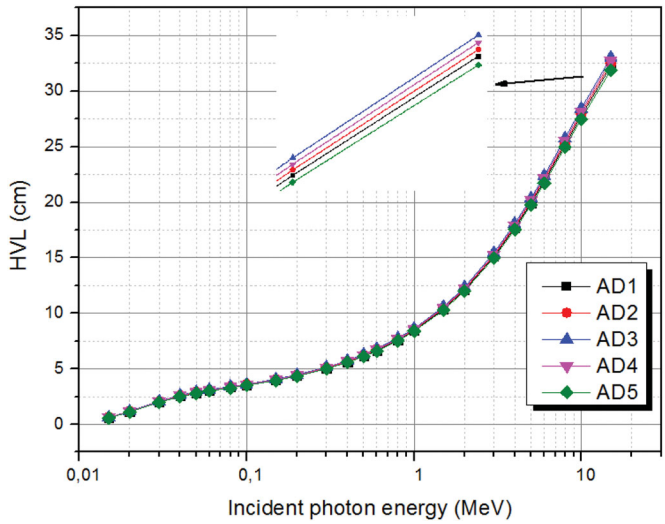

Figure 6. Comparison of HVL shielding values for all azadispiro samples with different contents in the energy range of 0.015–15 MeV.

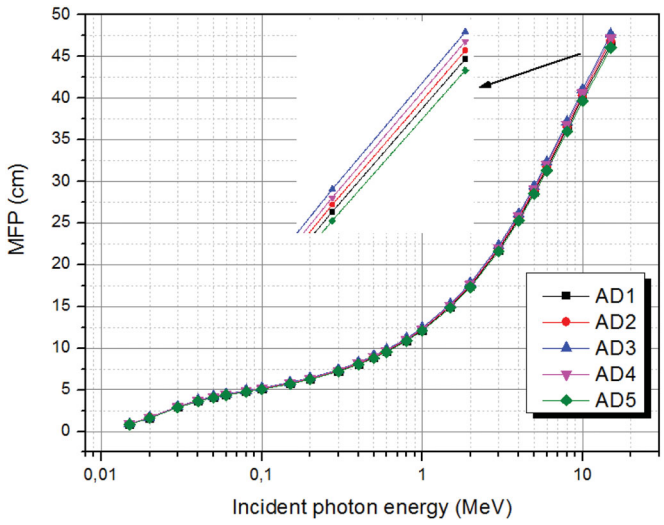

Figure 7. Comparison of MFP shielding values for all azadispiro samples with different contents in the energy range of 0.015–15 MeV.

Table 8. Equivalent atomic numbers of the azadispiro derivatives samples for the energy range 0.015–15 MeV.

Energy (MeV)	AD1	AD2	AD3	AD4	AD5
0.015	6.18	6.16	6.14	6.14	6.24
0.02	6.19	6.17	6.15	6.15	6.26
0.03	6.20	6.18	6.16	6.16	6.26
0.04	6.21	6.19	6.17	6.17	6.26
0.05	6.21	6.19	6.17	6.17	6.27
0.06	6.21	6.19	6.17	6.17	6.27
0.08	6.21	6.20	6.18	6.18	6.27
0.1	6.22	6.20	6.18	6.18	6.28
0.15	6.22	6.20	6.19	6.19	6.28
0.2	6.22	6.20	6.19	6.19	6.28
0.3	6.23	6.21	6.19	6.19	6.29
0.4	6.23	6.21	6.19	6.19	6.29
0.5	6.23	6.21	6.19	6.19	6.29
0.6	6.23	6.21	6.19	6.19	6.29
0.8	6.23	6.21	6.19	6.19	6.29
1	6.23	6.21	6.19	6.19	6.29
1.5	5.65	5.62	5.59	5.59	5.70
2	5.63	5.60	5.57	5.57	5.68
3	5.62	5.59	5.56	5.56	5.67
4	5.62	5.59	5.56	5.56	5.67
5	5.62	5.59	5.56	5.56	5.67
6	5.62	5.59	5.56	5.56	5.67
8	5.62	5.59	5.56	5.56	5.67
10	5.62	5.59	5.56	5.56	5.67
15	5.62	5.59	5.56	5.56	5.67

According to this graph, the increasing order of HVL values in all photon energy is observed as AD3 > AD4 > AD2 > AD1 > AD5. According to these results, it can be said that the AD5 sample has the highest radiation absorption capability, while the AD3 sample has the lowest radiation absorption capability.

MFP is also a substantial gamma radiation shielding parameter and is described as the average distance a photon travels between collisions with atoms of the target material. Figure 7 shows the variation of MFP values *vs.* the photon energy. This graph presents a change like Figure 6. However, as can be understood from Equations (12) and (13), MFP has higher values than HVL. This graph's behavior can be interpreted in a manner similar to the HVL.

The EBF of the azadispiro derivatives samples was calculated by using GP fitting parameters. Equivalent atomic number (Z_{eq}) values calculated using Equation (15) for these samples are displayed in Table 8. According to the table, the AD5 compound has the highest Zeq values while AD3 and AD4 have the smallest Zeq values. Figure 8(a–d) shows variations of the EBF in the energy range of 0.015–15 MeV at 1–40 mfp penetration depths. It is found from these graphs

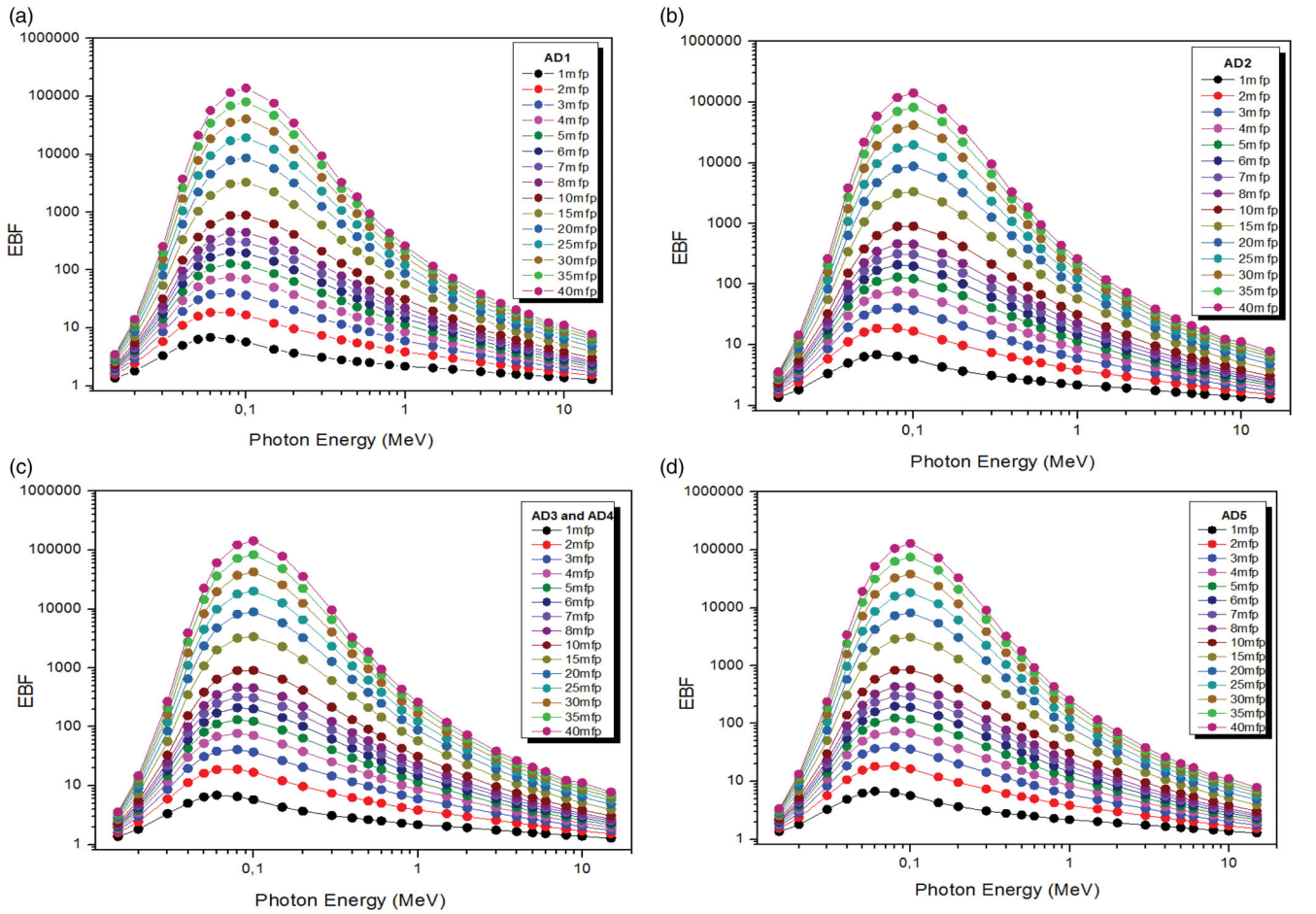

Figure 8. (a–d) Comparison of the exposure buildup factors EBF shielding values for all azadispiro samples with different contents in the energy range of 0.015–15 MeV.

that the EBF values of all samples at low and high energy regions are much lower when compared with the medium energy regions. In addition, Figure 9(a–c) show variations of the EBF in the different penetration depths at 0.015, 0.15, and 1.5 MeV. EBF shows wide variations at low energies and dependence on chemical compounds is at the highest level.

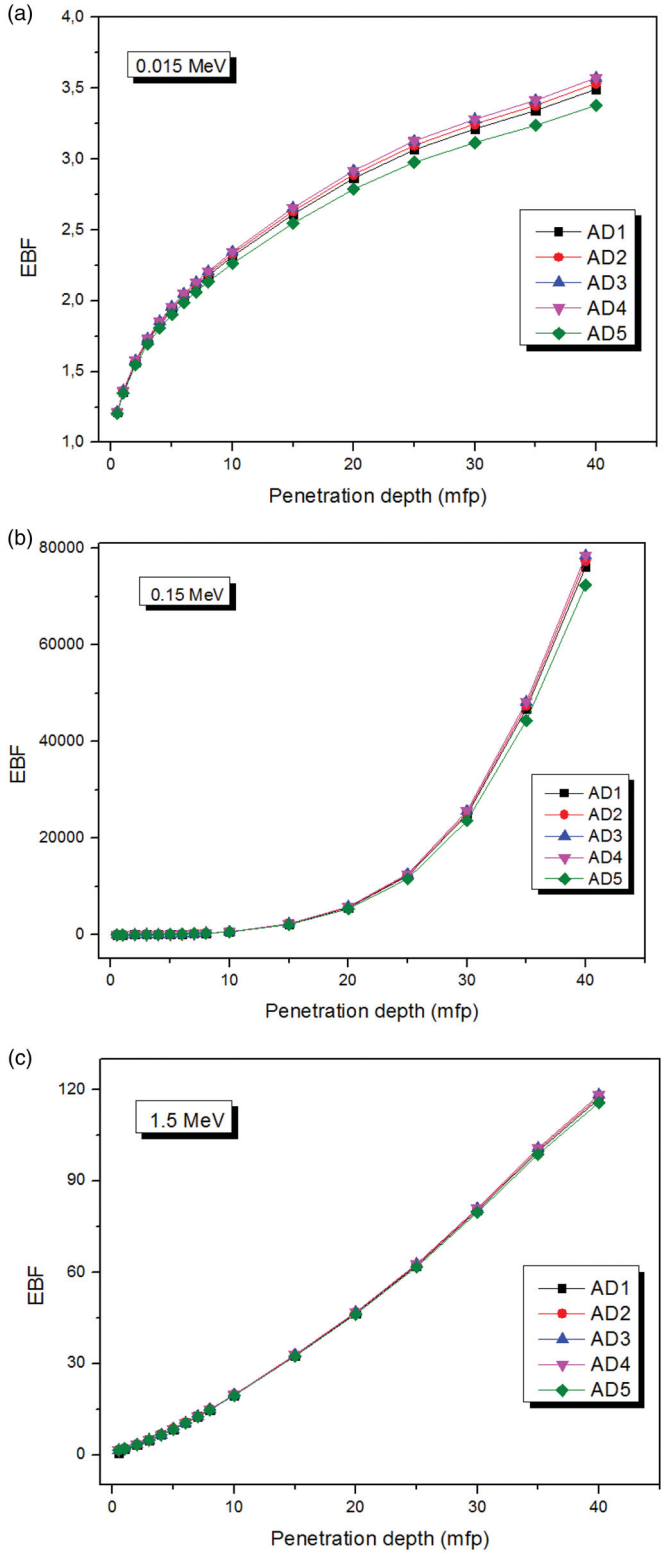

Figure 9. (a–c) Variations of the exposure buildup factors (EBF) in the different penetration depths.

It is observed that EBF values decrease as Z_{eq} values increase. At 1.5 MeV, since the dependence on chemical compounds starts to decrease, the EBF values of all compounds are almost the same. For all energies, the EBF values increase with the penetration depths. It is concluded that the EBF values of the AD5 compound are the lowest and have better gamma absorption performance according to the other azadispiro derivatives samples.

3.4. Ames/Salmonella assay

The Ames/*Salmonella* assay for the detection of test concentrations demonstrated that the 5 mM application dose exploited in the gamma and neutron radiation applications and the cytotoxic effects were not observed at this dose in any of the *Salmonella* test strains. Besides, genotoxicity assays showed that none of the azodispiro derivatives have genotoxic potential. In the current study, 5 different *Salmonella* test strains were carried out to test the genotoxic features of the azodispiro derivatives with their plenty of mechanisms, such as base substitutions, insertions, and deletions (Maron and Ames 1983; Turhan et al. 2014). Therefore, the azodispiro derivatives were genotoxically safe for the test doses in terms of genotoxic mechanisms.

4. Discussion

Currently, there are numerous radiation studies interested in an investigation of radiation protective properties of novel materials (glass, concrete, steel, etc.). Therefore, radiation research has been the center of attraction by scientists in various disciplines, such as agriculture, archeology, defense of military, nuclear energy and medicine, etc. because of its beneficial effects. In this regard, the present study aimed to study synthesized azadispiro derivatives have been analyzed of radiation absorption capacity and determined their potential to be exploited as substances for a drug be developed against radiation has been investigated. Neutron attenuation parameters, such as effective removal cross-section ΣR (cm^{-1}), MFP, HVL, and transmission number were theoretically determined by using the Monte Carlo simulation Geant4 code. The fact that a material has a high ΣR (cm^{-1}) value indicates that the material has a high rate of neutron-stopping ability (Singh et al. 2014). The low HVL and mean free path (λ) values show the neutron-stopping capacity of any material. These values show that new azadispiro derivatives have good neutron stopping power (Aygün et al. 2020a; Alaylar et al. 2021). Again, when the results are examined carefully, it can be clearly understood that the absorption parameters of azadispiro derivatives are not very low compared to the reference samples.

Accordingly, we can say whole azadispiro samples have excellent fast neutron absorption capability. It was determined that AD2, AD3, and AD4 samples have the highest absorption capacity among all Azadispiro derivatives. Consequently, It is demonstrated that all azadispiro derivatives have neutron absorption capabilities, and these samples can be used as active agents in anti-radiation drugs. Gamma

radiation shielding parameters, such as MAC, Z_{eff}, HVL, and MFP were calculated theoretically by using WinXCom software in the energy range from 0.015 to 15 MeV. MAC values, which are shielding parameters for gamma radiation, were calculated and it was found that MAC values for all samples decreased sharply due to the increase in photon energies in low-energy interaction areas.

These sharp decreases can be explained by the dominance of the photoelectric effect in the low energy region because the cross-section of the photoelectric effect changes depending on $Z^{4-5}/E^{3.5}$ and the photons either lose largely their energy or are entirely absorbed (Singh and Badiger 2016). Therefore, the MAC values in this region are significantly affected by the chemical composition of the sample. Since the chemical composition of the five synthesized samples used in this study is very close to each other, the variation of the MAC values with the increased photon energy is almost the same. However, we can say that decreased order of MAC values at low photon energy regions is observed as AD3 = AD4 < AD2 < AD1 < AD5. Here, since the chemical compositions of AD3 and AD4 compounds are the same, their MAC values are equal. In addition, it is seen from this graph that the decrease of the MAC values against increasing photon energy in the medium energy region is slower as the Compton scattering ($\propto 1/E$) event predominates (Ekinci et al. 2019; Issa et al. 2020). According to the results obtained, the AD5 compound has the highest radiation absorption capability when compared with other compounds. Z_{eff} is one of the most important gamma-ray shielding interactions, values of all samples were calculated and given in Figure 5. According to this graph, at 0.015 MeV, the Z_{eff} value for all compounds has a maximum value ranging from 5.53 to 5.69. After this, Z_{eff} values decrease up to 0.15 MeV exponentially as the incident photon energy increases because the photoelectric event dominates in the low energy region. Z_{eff} values of between 0.15 and 1 MeV have the lowest values that are nearly constant due to the dominance of the Compton scattering event in the intermediate energy region. In the energies higher than 1 MeV, Z_{eff} values increase slowly with the incident photon energy since in the high energy region where the pair production event is dominant, the cross-section of pair production changes depending on log(E). Hence, the Z_{eff} values vary highly depending on the incident photon energy. All samples have Zeef values as AD3 = AD4 < AD2 < AD1 < AD5. According to the greater the Z_{eff} value, the better the radiation-absorbing property. Therefore, the AD5 compound has the highest radiation absorption capability, while the AD3 or AD4 compound has the lowest radiation absorption capability. The Z_{eff} values of AD3 and AD4 compounds are the same because the Z_{eff} value also varies depending on the chemical composition of the sample. HVL values were calculated for all results are presented in Figure 6. According to this graph, the increasing order of HVL values in all photon energy is observed as AD3 > AD4 > AD2 > AD1 > AD5. The lower the HVL value, the better the material absorbs the radiation. Hence, the AD5 compound has the highest radiation absorption capability, while the AD3 compound has the lowest radiation absorption capability. EBF is an important parameter concerned with the exposure of gamma photons in the air after penetrating the thickness of the investigated material (Rammah et al. 2020). It is seen from these Figure 8(a–d) that EBF values of all compounds in low and high energy regions are much lower when compared with the medium energy regions because the photoelectric event and pair production event dominate in these energy regions. In these events, photons are either entirely absorbed or seriously lose their energies. In the medium energy region where the Compton scattering event prevails, EBF values slowly increase and reach maximum values since in that event, decreased photons energies give rise to the buildup of photons. These maximum EBF values are around 0.06–0.1 MeV for all samples. According to these results, it can be said that the EBF values of the AD5 sample are the lowest and have better gamma absorption performance according to the other azadispiro derivatives samples. Five different *Salmonella* test strains were carried out to test the genotoxic features of the azodispiro derivative samples. the cytotoxic effects were not observed at this 5 mM dose of any of the *Salmonella* test strains. According to these results, it determined that genotoxicity assays showed that none of the azodispiro derivatives have genotoxic potential.

5. Conclusions

In this paper, five different types of synthesized azadispiro derivatives have been analyzed with their radiation absorption capacity. Hence, important fast neutron absorption parameters were theoretically determined by using the Geant4 code. The neutron absorption dose measurements were made. Both theoretically and experimental results are shown that these azidispiro derivatives have good neutron absorption capacities according to the like paraffin and high-density propylene. It was observed that, among all azidispiro derivatives, AD2, AD3, and AD4 have high neutron absorption capacity. Gamma-ray attenuation parameters were figured out in the energy range from 0.015 to 15 MeV with the WinXCom program to determine the gamma-attenuation capacity of samples. According to calculated results, all azidispiro samples have gamma-ray absorption ability. But it was seen that AD1 and AD5 have high absorption capacities among all azidispiro samples. In addition, it determined genotoxicity safe properties, and it was found that these azidispiro samples do not have any toxicity effect. So, it is shown that these samples can use in the production of any antiradiation drugs.

Disclosure statement

No potential conflict of interest was reported by the author(s).

Funding

The author(s) reported there is no funding associated with the work featured in this article.

Notes on contributors

Burak Alaylar, Ph.D., is an Assistant Professor, Department of Molecular Biology and Genetics, Faculty of Sciences and Arts, Agri Ibrahim Cecen University, Agri, Turkey.

Bünyamin Aygün, Ph.D., is an Associate Professor, Department of Electronics and Automation, Vocational School, Agri Ibrahim Cecen University, Agri, Turkey.

Kadir Turhan, Ph.D., is an Associate Professor, Department of Chemistry, Faculty of Art and Sciences, Yildiz Technical University, Istanbul, Turkey.

Mehmet Karadayı, Ph.D., is an Assistant Professor, Department Biology, Faculty of Science, Ataturk University, Erzurum, Turkey.

Esra Cinan, Ph.D., Research Assistant, Department of Physics, Faculty of Sciences, Ataturk University, Erzurum, Turkey.

Zuhal Turgut, Ph.D., is a Professor, Department of Chemistry, Faculty of Art and Sciences, Yildiz Technical University, Istanbul, Turkey.

Gökçe Karadayı, is an Assistant Professor, Department of Molecular Biology and Genetics, Faculty of Sciences, Ataturk University, Erzurum, Turkey.

Mohammed Ibrahim Abu Al-Sayyed, Ph.D., is an Assistant Professor, Department of Physics, Faculty of Science, Isra University, Amman, Jordan and Department of Nuclear Medicine Research, Institute for Research and Medical Consultations, Imam Abdulrahman bin Faisal University, Damman, Saudi Arabia.

Medine Güllüce, Ph.D., is a Professor, Department of Biology, Faculty of Science, Ataturk University, Erzurum, Turkey.

Abdulhalik Karabulut, Ph.D., is a Professor, Department of Physics, Faculty of Sciences, Ataturk University, Erzurum, Turkey.

ORCID

Burak Alaylar http://orcid.org/0000-0001-6737-3440
Bünyamin Aygün http://orcid.org/0000-0002-9384-1540
Kadir Turhan http://orcid.org/0000-0002-7718-1618
Mehmet Karadayı http://orcid.org/0000-0002-2473-0409
Medine Güllüce http://orcid.org/0000-0002-5957-8259

References

Alaylar B, Aygün B, Turhan K, Karadayi G, Şakar E, Singh VP, Sayyed MI, Pelit E, Karabulut A, Güllüce M, et al. 2021. Characterization of gamma-ray and neutron radiation absorption properties of synthesized quinoline derivatives and their genotoxic potential. Radiat Phys Chem. 184:109174.

Al Houari G, Kerbal A, Bennani B, Baba MF, Daoudi M, Hadda TB. 2008. Drug design of new antitubercular agents: 1,3-dipolar cycloaddition reaction of para-substituted-benzadoximes and 3-para-methoxy-benzyliden-isochroman-4-ones. Arkivoc. 2008(12):42–50.

Amani F, Allahbakhshian Farsani M, Gholami M, Aghamiri SMR, Bakhshandeh M, Hossein Mohammadi M. 2021. The protective effect of oleuropein against radiation-induced cytotoxicity, apoptosis, and genetic damage in cultured human lymphocytes. Int J Radiat Biol. 97(2):179–193.

Aygün B, Korkut T, Karabulut A, Gencel O, Karabulut A. 2015. Production and neutron irradiation tests on a new epoxy/molybdenum composite. Int J Polym Anal Charact. 20(4):323–329.

Aygün B, Şakar E, Korkut T, Sayyed MI, Karabulut A, Zaid MHM. 2019. Fabrication of Ni, Cr, W reinforced new high alloyed stainless steels for radiation shielding applications. Results Phys. 12:1–6.

Aygün B, Şakar E, Singh VP, Sayyed MI, Korkut T, Karabulut A. 2020a. Experimental and Monte Carlo simulation study on potential new composite materials to moderate neutron-gamma radiation. Prog Nucl Energy. 130:103538.

Aygün B, Şakar E, Cinan E, Yorgun NY, Sayyed MI, Agar O, Karabulut A. 2020b. Development and production of metal oxide doped glasses for gamma ray and fast neutron shielding. Radiat Phys Chem. 174:108897.

Aygün B, Şakar E, Agar O, Sayyed MI, Karabulut A, Singh VP. 2021a. Development of new heavy concretes containing chrome-ore for nuclear radiation shielding applications. Prog Nucl Energy. 133:103645.

Aygün B, Alaylar B, Akıncıoğlu A, Alım B, Kocaman ET, Karadayı M, Abu Al-Sayyed MI, Aksu Ş, Şakar E, Özpolat ÖF, et al. 2021b. Determination of radioprotective and genotoxic properties of sulfamide derivatives. Radiochim Acta. 109(12):891–904.

Aygün B, Alaylar B, Turhan K, Şakar E, Karadayı M, Sayyed MI, Pelit E, Güllüce M, Karabulut A, Turgut Z, et al. 2021c. Investigation of neutron and gamma radiation protective characteristics of synthesized quinoline derivatives. Int J Radiat Biol. 96(11):1423–1434.

Biswas R, Sahadath H, Mollah AS, Huq MF. 2016. Calculation of gamma-ray attenuation parameters for locally developed shielding material: polyboron. J Radiat Res Appl Sci. 9(1):26–34.

Das P, Boone S, Mitra D, Turner L, Tandon R, Raucher D, Hamme AT. 2020. Synthesis and biological evaluation of fluoro-substituted spiro-isoxazolines as potential anti-viral and anti-cancer agents. RSC Adv. 10(50):30223–30237.

Dauer LT, Ainsbury EA, Dynlacht J, Hoel D, Klein BEK, Mayer D, Prescott CR, Thornton RH, Vano E, Woloschak GE, et al. 2017. Guidance on radiation dose limits for the lens of the eye: Overview of the recommendations in NCRP commentary no. 26. Int J Radiat Biol. 93(10):1015–1023.

Ekinci N, Kavaz E, Aygün B, Perişanoğlu U. 2019. Gamma ray shielding capabilities of rhenium-based superalloys. Radiat Eff Defects Solids. 174(5–6):435–451.

El-Khayatt AM, El-Sayed Abdo A. 2009. MERCSF-N: a program for the calculation of fast neutron removal cross sections in composite shields. Ann Nucl Energy. 36(6):832–836.

Erugu Y, Sangepu B, Varre K, Pamanji R, Bomma Y, Janapala VR, Srinivasarao V, Tigulla PP, Jetti VR, Rao Jonapala V, et al. 2014. Design, an efficient ecofriendly synthesis of spirooxindole derivatives and their anticancer activity supported by molecular docking studies. World J Pharm Sci. 3(8):1895–1914.

Feng T, Ye R, Zhuang H, Rong Z, Fang Z, Wang Y, Gu Z, Jin Z. 2013. Physicochemical properties and sensory evaluation of Mesona Blumes gum/rice starch mixed gels as fat-substitutes in Chinese Cantonese-style sausage. Food Res Int. 50(1):85–93.

Gerward L, Guilbert N, Jensen KB, Levring H. 2004. WinXCom – a program for calculating X-ray attenuation coefficients. Radiat Phys Chem. 71(3–4):653–654.

Issa SAM, Rashad M, Zakaly HMH, Tekin HO, Abouhaswa AS. 2020. Nb_2O_5-Li_2O-Bi_2O_3-B_2O_3 novel glassy system: evaluation of optical, mechanical, and gamma shielding parameters. J Mater Sci: Mater Electron. 31(24):22039–22056.

Kaewkhao J, Korkut T, Korkut H, Aygün B, Yasaka P, Tuscharoen S, Insiripong S, Karabulut A. 2017. Monte Carlo design and experiments on the neutron shielding performances of B_2O_3–ZnO–Bi_2O_3 glass system. Glass Phys Chem. 43(6):560–563.

Kamiński K, Obniska J, Dybała M. 2008. Synthesis, physicochemical and anticonvulsant properties of new N-phenylamino derivatives of 2-azaspiro[4.4]nonane- and [4.5]decane-1,3-diones: part V. Eur J Med Chem. 43(1):53–61.

Kesharwani S, Sahu NK, Kohli DV. 2009. Synthesis and biological evaluation of some new spiro derivatives of barbituric acid. Pharm Chem J. 43(6):315–319.

Lamarsh JR, Baratta AJ. 2001. Introduction to nuclear engineering. 3rd ed. New Jersey (US): Prentice Hall; p. 1–810.

Maron D, Ames BN. 1983. Revised methods for the *Salmonella* mutagenicity test. Mutat Res. 113(3–4):173–215.

McAlister DR. 2016. Neutron shielding materials. University Lane Lisle (US): PG Research Foundation, Inc.; p. 1–16.

More CV, Alsayed Z, Badawi MS, Thabet AA, Pawar PP. 2021. Polymeric composite materials for radiation shielding: a review. Environ Chem Lett. 19(3):2057–2090.

Mortelmans K, Zeiger E. 2000. The Ames *Salmonella*/microsome mutagenicity assay. Mutat Res. 455(1–2):29–60.

Rammah YS, Mahmoud KA, Sayyed MI, El-Agawany FI, El-Mallawany R. 2020. Novel vanadyl lead-phosphate glasses: P_2O_5–PbO–ZnO–Na_2O–V_2O_5: synthesis, optical, physical and gamma photon attenuation properties. J Non Cryst Solids. 534: 19318–19327.

Reddy DM, Qazi NA, Sawant SD, Bandey AH, Srinivas J, Shankar M, Singh SK, Verma M, Chashoo G, Saxena A, et al. 2011. Design and synthesis of spiro derivatives of parthenin as novel anti-cancer agents. Eur J Med Chem. 46(8):3210–3217.

Şakar E, Ozpolat OF, Alım B, Sayyed MI, Kurudirek M. 2020. Phy-X/PSD: development of a user friendly online software for calculation of parameters relevant to radiation shielding and dosimetry. Radiat Phys Chem. 166:108496.

Sayyed MI, AlZaatreh MY, Dong MG, Zaid MHM, Matori KA, Tekin HO. 2017. A comprehensive study of the energy absorption and exposure buildup factors of different bricks for gamma-rays shielding. Results Phys. 7:2528–2533.

Sayyed MI, Lakshminarayana G. 2018. Structural, thermal, optical features and shielding parameters investigations of optical glasses for gamma radiation shielding and defense applications. J Non Cryst Solids. 487:53–59.

Schober H. 2014. An introduction to the theory of nuclear neutron scattering in condensed matter. J Neutron Res. 17(3–4):109–357.

Singh MP, Sandhu BS, Singh B. 2007. Measurement of effective atomic number of composite materials using scattering of γ-rays. Nucl Instrum Methods Phys Res A. 580(1):50–53.

Singh VP, Badiger NM, Chanthima N, Kaewkhao J. 2014. Evaluation of gamma-ray exposure buildup factors and neutron shielding for bismuth borosilicate glasses. Radiat Phys Chem. 98:14–21.

Singh VP, Badiger NM. 2016. Photon interaction with semiconductor and scintillation detectors. Nucl Sci Tech. 27(3):185–191.

Srivastava K, Lakhmani D, Srivasatava J, Singh RB. 2020. Synthesis and characterization of new thiazole involving isatin for studying their antimicrobial activity. Indian J Chem Sect B. 59(4):485–487.

Tan X, Liu P, Guo DH. 2016. Anti-radiation drugs for radiotherapy: research advances. J Int Pharm Res. 43(5):870–875.

Tang W, Shen M, Xie J, Liu D, Du M, Lin L, Gao H, Hamaker BR, Xie M. 2017. Physicochemical characterization, antioxidant activity of polysaccharides from *Mesona chinensis* Benth and their protective effect on injured NCTC-1469 cells induced by H_2O_2. Carbohydr Polym. 175:538–546.

Tellili B, Elmahroug Y, Souga C. 2014. Calculation of fast neutron removal cross sections for different lunar soils. Adv Space Res. 53(2):348–352.

Thadhaney B, Sain D, Pemawat G, Talesara GL. 2010. Synthesis and antimicrobial evaluation of ethoxyphthalimide derivatized spiro [indole3,5′-(1,3)thiazolo(4,5-c)isoxazol]-2(1*H*)-ones via ring closure metathesis. Indian J Chem Sect B. 49(30):368–373.

Tsoulfanidis N. 1984. Computational methods in reactor shielding. Nucl Technol. 13(10):449–1982.

Tuğcu FT, Turhan K, Karadayi M, Güllüce M. 2018. Synthesis of 4-thiazolidinone derivatives and assessment of their toxicological properties. Rom Biotechnol Lett. 23:13276–13286.

Turhan K, Ozturkcan SA, Turgut Z, Karadayi M, Gulluce M. 2012. Protective properties of five newly synthesized cyclic compounds against sodium azide and *N*-methyl-*N*′-nitro-*N*-nitrosoguanidine genotoxicity. Toxicol Ind Health. 28(7):605–613.

Turhan K, Ozturkcan SA, Turgut Z, Karadayi M, Aslan A, Gulluce M. 2014. Genotoxic and antigenotoxic assessment of four newly synthesized dihydropyridine derivatives. Toxicol Ind Health. 30(3): 275–783.

USNRC. 2017. NRC: uses of radiation. Washington, DC (US): USNRC.

Wang W, Xue C, Mao X. 2020. Radioprotective effects and mechanisms of animal, plant and microbial polysaccharides. Int J Biol Macromol. 15(153):373–384.

Yoshikawa S, Hareyama N, Ikeda K, Kurokawa T, Nakajima M, Nakao K, Mochizuki H, Ichinose H. 2009. Effects of TRK-820, a selective kappa opioid receptor agonist, on rat schizophrenia models. Eur J Pharmacol. 606(1–3):102–108.

Youssef MM, Amin MA. 2010. Microwave assisted synthesis of some new heterocyclic spiro-derivatives with potential antimicrobial and antioxidant activity. Molecules. 15(12):8827–8840.

Zaher AF, Khalil NA, Ahmed EM. 2010. Synthesis and anticonvulsant activity of new 3′-aryl-7-bromo-spiro[[1]benzothiophene-3,2′-[1,3] thiazolidine]-24'-dione derivatives. Orient J Chem. 26(4):1241–1248.

Zali NM, Yazid H, Megat Ahmad MHAR. 2018. Neutron shielding behavior of thermoplastic natural rubber/boron carbide composites. Mater Sci Eng. 298:1–5.